

NASA TECHNICAL NOTE



NASA TN D-6096

e. 1

NASA TN D-6096

LOAN COPY: RETURN
AFWL (WLOL)
KIRTLAND AFB, N ME

0132956



TECH LIBRARY KAFB, NM

TRANSIENT PERFORMANCE OF A TURBOALTERNATOR GAS-BEARING SYSTEM

*by James C. Wood, Joseph S. Curreri,
and Armen S. Asadourian*

*Lewis Research Center
Cleveland, Ohio 44135*

NATIONAL AERONAUTICS AND SPACE ADMINISTRATION • WASHINGTON, D. C. • NOVEMBER 1970



0132956

1. Report No. NASA TN D-6096		2. Government Accession No.		3. Recipie 0132956	
4. Title and Subtitle TRANSIENT PERFORMANCE OF A TURBOALTERNATOR GAS-BEARING SYSTEM				5. Report Date November 1970	
7. Author(s) James C. Wood, Joseph S. Curreri, and Armen S. Asadourian				6. Performing Organization Code	
9. Performing Organization Name and Address Lewis Research Center National Aeronautics and Space Administration Cleveland, Ohio 44135				8. Performing Organization Report No. E-5820	
12. Sponsoring Agency Name and Address National Aeronautics and Space Administration Washington, D. C. 20546				10. Work Unit No. 120-27	
15. Supplementary Notes				11. Contract or Grant No.	
16. Abstract The results of experimental operation of a gas-bearing turboalternator under transient tests are presented. The tests were rapid startup, change in operational mode of the thrust bearing, and stepping of the electrical load using two types of turboalternator speed control. The journal bearing exceeded the design clearance limits during the startup test, but operated stably. The excessive clearance was caused by insufficient control of the coolant through the bearing mount. The thrust bearing experienced large changes during the electrical load steps using one method of speed control but also always operated stably.				13. Type of Report and Period Covered Technical Note	
17. Key Words (Suggested by Author(s)) Brayton cycle Thrust bearing Gas bearings Turboalternator Journal bearing Transient				14. Sponsoring Agency Code	
18. Distribution Statement Unclassified - unlimited					
19. Security Classif. (of this report) Unclassified		20. Security Classif. (of this page) Unclassified		21. No. of Pages 24	22. Price* \$3.00

TRANSIENT PERFORMANCE OF A TURBOALTERNATOR GAS-BEARING SYSTEM

by James C. Wood, Joseph S. Curreri, and Armen S. Asadourian

Lewis Research Center

SUMMARY

The results of experimental operation of a gas-bearing turboalternator under various transient tests are presented in this report. The tests performed were rapid startup, change in operational mode of the thrust bearing, and stepping of the electrical load with two types of shaft speed control. These tests are representative of the condition that may be found in an actual space-power system.

During the startup tests, the turboalternator journal bearing clearance exceeded the design limits but operated stably. The excessive clearance was caused by insufficient control of the coolant through the bearing mount ring.

The thrust bearing experienced large clearance changes during the alternator step-load transients. This was due to the method of speed control. The transient from hydrostatic to hydrodynamic operation on the thrust bearing took place smoothly.

INTRODUCTION

As part of Lewis Research Center's work in developing space-power generation systems, studies were made (refs. 1 and 2) and hardware was built for a power system operating on the Brayton thermodynamic cycle with argon as the working fluid. As part of the work, a turbine-driven alternator (turboalternator) incorporating self-acting gas-lubricated bearings was built (refs. 3 to 6).

Extensive testing was conducted on the turboalternator and its components. The results of the testing done on the turbine are reported in references 7 to 10. The operating characteristics of the alternator and the associated electrical control systems are presented in references 11 to 17. The performance of the turboalternator is presented in references 18 and 19.

Of prime importance in the development of the turboalternator is the operation of the gas bearings during transient and steady-state operation. The steady-state tests of

the gas bearings at Lewis is discussed in reference 20. The results of the transient tests are contained herein.

The results discussed include the effects of a rapid turboalternator startup from zero speed and 580⁰ F (580 K) to design speed and approximately 1150⁰ F (896 K), a change in the operating mode of the thrust bearing from hydrostatic (externally pressurized) operation to hydrodynamic (self-acting) operation, and the effects of stepping the electrical load using two types of turboalternator shaft speed control. These particular tests are important because of the possibility of transients starting a mode of unstable operation that could lead to a catastrophic bearing failure.

APPARATUS

Turboalternator Description

The turboalternator consists of a four-pole homopolar inductor alternator and a two-stage axial-flow turbine mounted on a common shaft. The shaft is supported on two self-acting (hydrodynamic) tilting-pad journal bearings and an inward-pumping, spiral-groove, self-acting thrust bearing. The turboalternator is shown in figure 1. Table I lists the design conditions.

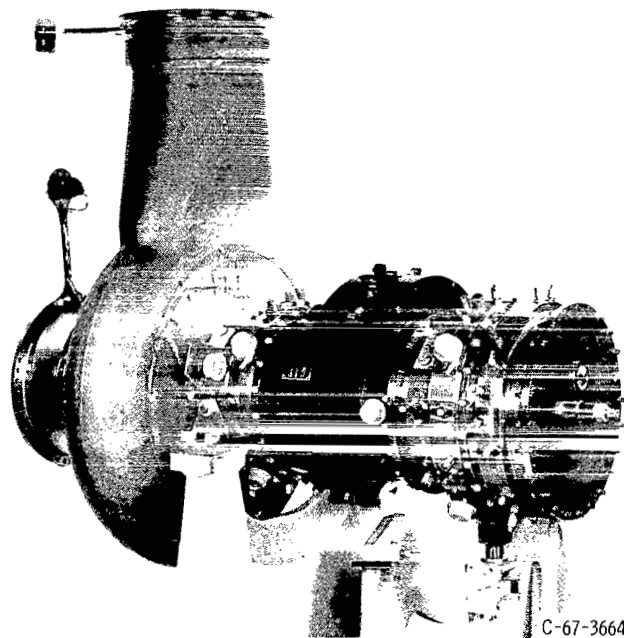


Figure 1. - Turboalternator.

TABLE I. - DESIGN CONDITIONS

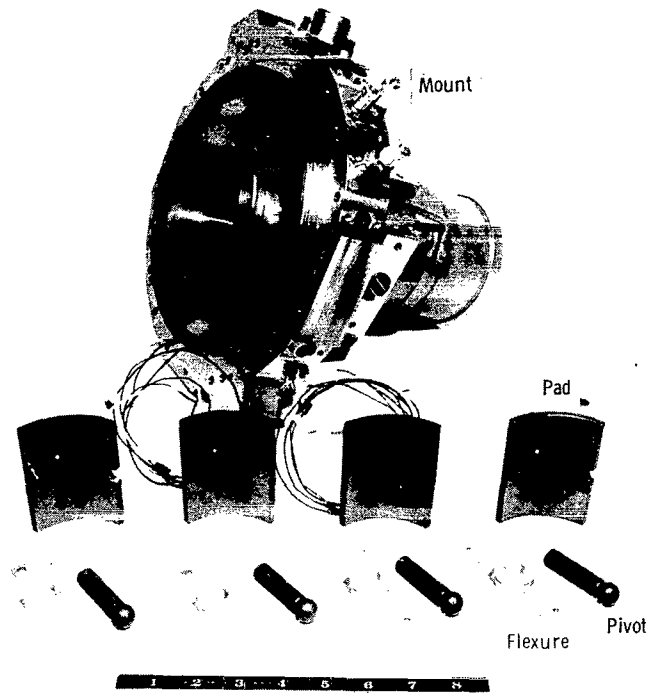
Turbine:	
Inlet total temperature, °F (K)	1225 (936)
Inlet total pressure, psia (N/m ²)	8.45 (5.82×10 ⁴)
Pressure ratio, total to static	1.26
Rotative speed, rpm	12 000
Coolant flow rates, lb/min (kg/min):	
Front journal-bearing (forward) heat exchanger	3.6 (1.63)
Front journal-bearing (rear) heat exchanger	1.5 (0.68)
Front journal-bearing support ring heat exchanger	1.5 (0.68)
Rear journal-bearing (forward) heat exchanger	1.7 (0.77)
Rear journal-bearing (rear) heat exchanger	0.4 (0.18)
Rear journal-bearing support ring heat exchanger	0
Thrust-bearing heat exchanger	1.7 (0.77)

The journal bearings are located between the turbine and alternator and between the alternator and thrust bearing. Each bearing consists of four pads; and each pad covers an 80° arc of the shaft circumference. The pads pivot on a nonconforming ball and socket (pivot ball diameter, 0.625 in. (1.58 cm); socket diameter, 0.812 in. (2.06 cm)). The pivot ball is mounted to the bearing housing by a flexible beam (flexure). The flexures reduce the rigid-body critical speeds of the rotor bearing system and provide accommodation for thermal growth. The pivots allow angular motion of the pads thus providing good alinement capability. The bearing parts are shown in figure 2.

Although the journal bearings are designed to be self-acting, they also can be externally pressurized (hydrostatic). External pressurization is used for rotational starting and stopping when the shaft is in a position other than vertical.

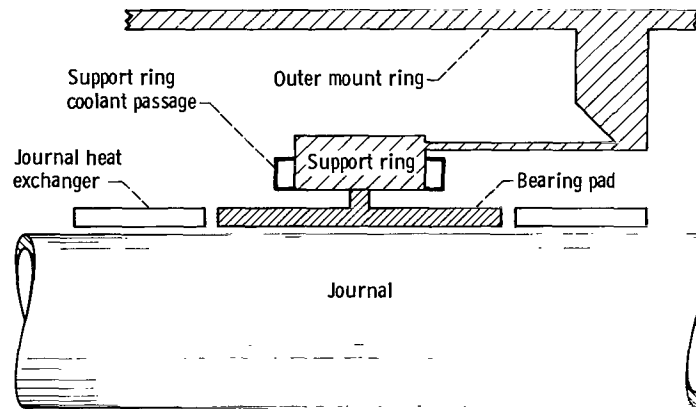
The heat generated in the journal bearings is removed by liquid cooled heat-exchanger sleeves located around the shaft on each side of the bearings. (The coolant used in the test was Dow Corning 200.) The heat is conducted from the shaft to the heat exchangers through a 0.005-inch (1.27×10⁻²-cm) radial gap. The inner surface of the shaft under the journal-bearing area is plated with a 0.125-inch (0.318-cm) thick layer of copper. The plating is used to maintain uniform temperatures along the shaft under the bearing pads for minimum thermal gradient and hence minimum distortion in the bearing. A schematic drawing of the journal bearing and heat exchangers is shown in figure 3.

The support ring, holding the bearing assembly, contains liquid coolant passages to allow for bearing clearance adjustment during operation. Since the temperature of the support ring is largely determined by the coolant temperature, adjustment of coolant



C-69-485

Figure 2. - Parts layout for front journal-bearing assembly.



CD-10553-15

Figure 3. - Schematic of journal bearing.

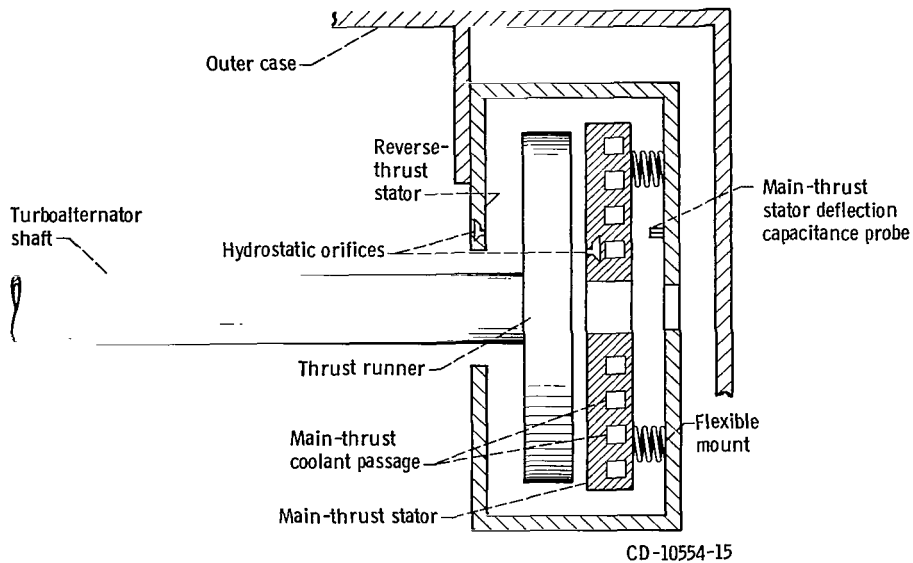
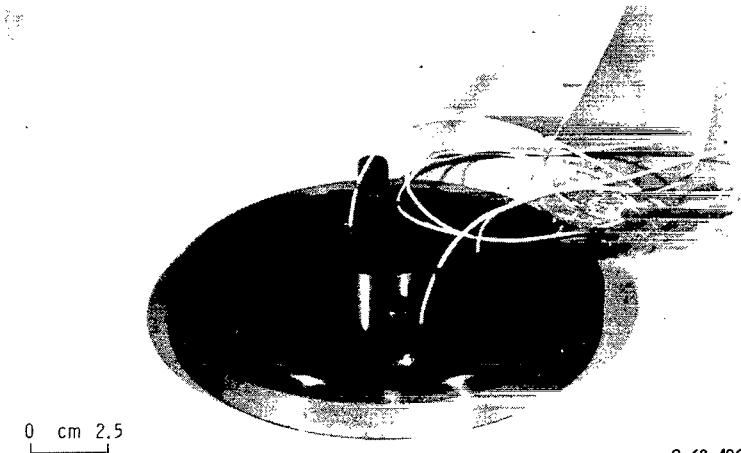
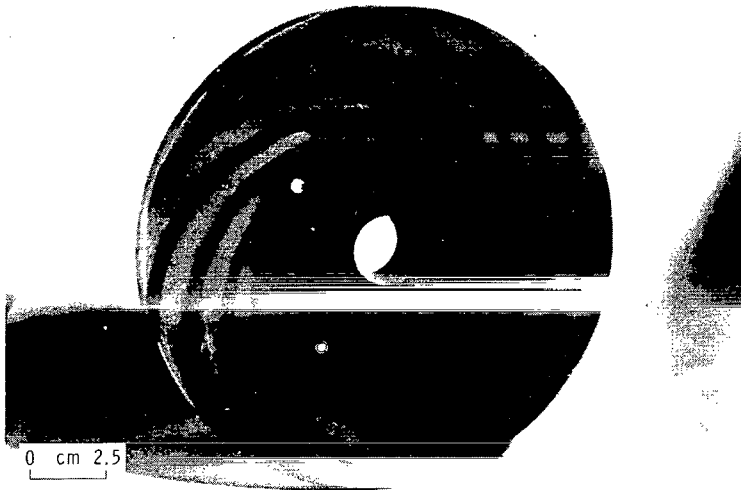


Figure 4. - Schematic thrust bearing.

temperature results in a bearing clearance adjustment.

A schematic view of the thrust bearing is shown in figure 4. Both the main and reverse thrust bearings can be operated hydrostatically, but only the main thrust bearing can be operated hydrodynamically. The hydrostatic capability is for use during rotational starting and stopping. The thrust load on the main bearing is 87 pounds (390 N) when the turboalternator is in the vertical position and at the turbine design condition. Of this, 57 pounds (26 kg) is shaft mass and 30 pounds (135 N) is aerodynamic forces. The main thrust bearing is designed for a maximum 250-pound (1100-N) load to provide for transient loads encountered in startup. The main-thrust-bearing stator (fig. 5) is flexibly mounted to permit dynamic alinement of the stator with the thrust runner. Liquid flows through the main thrust stator to cool it. Details of thrust-bearing design are presented in reference 4.

A small amount of argon at ambient temperature is fed through the turboalternator from the thrust-bearing end of the machine. The gas flows through and around the shaft toward the turbine end (fig. 6). The gas then enters the main gas flow through gap passages before and after the turbine. The purpose of the gas is to prevent backflow of hot turbine gas into the bearing area and to assist in heat removal. The cooling argon was obtained from a source external to the closed loop (see fig. 7). In a space-power system, this gas supply would be bled from the discharge of the argon-circulating compressor.



C-69-486

Figure 5. - Main-thrust-bearing stator.

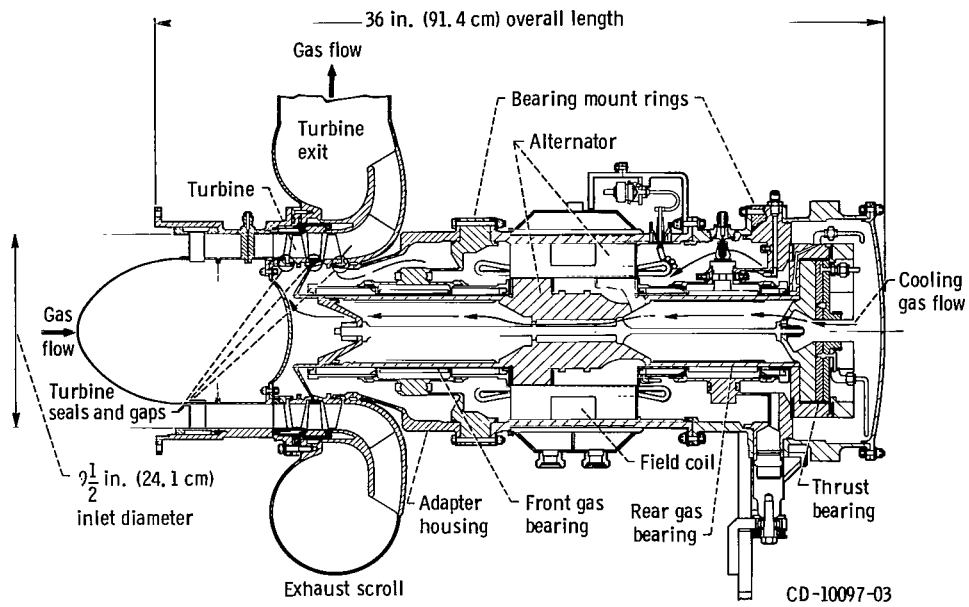


Figure 6. - Cross-sectional view of turboalternator.

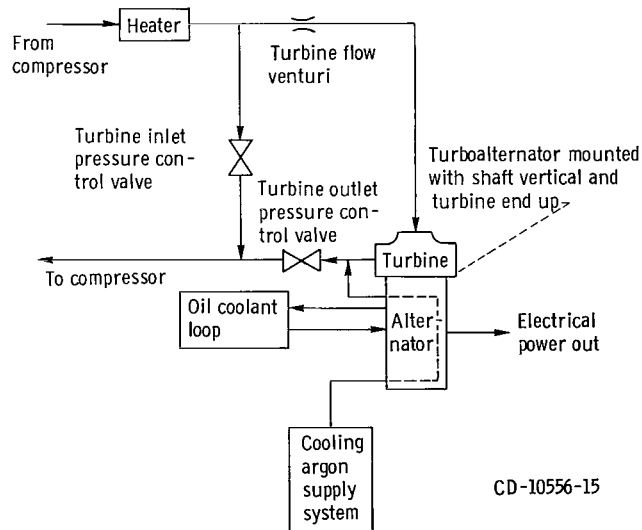


Figure 7. - Schematic Brayton cycle turboalternator test facility.

Test Facility Description

The test facility used to operate the turboalternator is described in detail in reference 19. The facility is a closed loop, using a motordriven compressor to circulate the argon. A flow schematic is shown in figure 7.

The argon supplied to the turbine was heated by the electric heater. Inlet pressure was controlled by regulating the flow through the turbine bypass. Turbine weight flow was measured by the venturi upstream of the turboalternator, and pressure ratio was controlled by the valve at the turbine discharge. This control valve was also used to automatically control turbine speed for some of the tests.

The oil loop supplied coolant to the alternator-stator heat exchangers and to the bearing support ring at each of the bearings. Coolant temperatures and the oil flow rates to the alternator, bearing heat exchangers, and support rings could be controlled individually.

The alternator electrical output was absorbed by the electrical system shown in figure 8. This system is like the one that would be used in an actual space-power

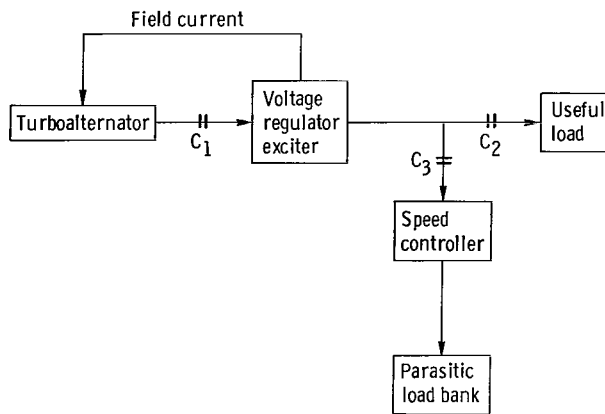


Figure 8 - Schematic of turboalternator electrical system.

system. In the actual system, the turboalternator would run at constant power with the power going to the parasitic load and the useful load. The useful load represents the user demand. The speed controller maintains a constant turboalternator speed by controlling the amount of power to the parasitic loads as the useful load changes.

The voltage-exciter was designed and built for NASA under the same contract as the turboalternator. Two regulator-exciter were built; one a breadboard model and the other a flight-type design. The breadboard model was used in these tests because adjustments, if necessary, could be made.

The electric speed controller used is a static breadboard type. It was designed and built at Lewis specifically for this system. Speed is controlled within the desired range by phase-controlled parasitic loading of the alternator. This type of control eliminates control valves in the gas system, but it causes some undesirable effects (ref. 21) in the electrical system. The control range was 394 to 408 hertz (11 820 to 12 240 rpm) for rated system conditions.

Instrument Description

Chromel-Alumel thermocouples were used to measure turboalternator internal temperatures and turbine inlet and outlet gas temperatures. The inlet and outlet gas temperatures were measured with bare spike stream thermocouples mounted on rakes. The oil coolant temperatures were measured with iron-constantan thermocouples immersed in the oil stream.

Pressures were measured with strain-gage transducers. Static and total pressures were measured at the turbine inlet and outlet. Turboalternator case pressures were also measured.

The turbine weight flow was measured with a calibrated venturi, coolant oil flow with turbine flowmeters, and coolant gas flows with rotameters.

Capacitance probes were used to measure journal motion relative to the housing, thrust-bearing film thickness, film thickness between each bearing pad and the shaft, and the dynamic motion of the bearing pads relative to the turboalternator housing.

The output of the probe is a voltage that is directly proportional to the clearance. All the outputs of the capacitance probes were recorded on an FM magnetic tape recorder. These data were later put on a chart recorder or played back on oscilloscopes where the traces were photographed. The outputs of the bearing clearance probes were also sent to oscilloscopes during the tests for continuous monitoring. The wattmeters, voltmeters, and ammeters used to measure alternator output were the wide-frequency-range, true-rms electronic types.

DISCUSSION OF RESULTS

This report contains the results of three of the dynamic tests performed on the turboalternator and how they affected the gas bearings. The tests were the turboalternator startup transients from zero speed and 580^o F (580 K) up to design speed and 1145^o F (895 K), change in thrust bearing operational mode, and stepping of the electrical load. The tests will be discussed separately.

Startup Transients

This test was performed to determine the effects of a rapid startup on the rotor-bearing system. The effects include those of the shaft acceleration from zero to design speed (12 000 rpm) and the thermal transient from a 580^o F (580 K) to a 1145^o F (895 K) turbine inlet temperature. The first portion of the test showed how the rotor-bearing system reacted to initial shaft rotation until the journal bearings were operating in a hydrodynamic mode and they had accelerated past the first two critical speeds. It also showed how the electric speed control reacted in stopping speed acceleration and controlling it at 12 000 rpm. The second portion showed how the bearing clearances were affected by thermal growth. Of special interest was the front journal bearing because of its proximity to the turbine.

In order to get as fast a thermal transient as possible, the turboalternator was shut down while it was still hot and before the startup test; it cooled while the facility piping was kept as hot as possible. The cooling was accomplished by removing the insulation from the turbine and not the adjacent piping. The insulation was then replaced immediately before the startup.

The coolant-oil-flow and temperature-limit controls were set at the values required to maintain nominal bearing clearance at turboalternator design conditions. These conditions are specified in table I. The thrust bearing was operated in the hydrostatic mode.

The electrical output of the alternator was connected to the parasitic speed control through the voltage regulator-exciter. No useful loading was used for the test. The entire power output was absorbed by the parasitic load bank.

At the beginning of the test, the facility heater was turned on full, the coolant oil system was started, and the turbine outlet valve was opened to the point where design pressure ratio (1.26) was established across the turbine. Turbine inlet pressure was maintained at the design value of 8.45 psia (58 kN/m²) by the automatic control.

The acceleration of the shaft from 0 to 12 000 rpm and the bearing clearance during that time interval are shown in figure 9. The clearance plotted is the average radial clearance of the front journal bearing. The rear journal showed the same characteristics so it is not plotted. The curve shows that for the turbine design inlet pressure and pressure ratio, the shaft reached design speed in 12 seconds. The electric speed controller started to load the alternator at about 11 800 rpm and held the speed at 12 000 rpm without going into an oscillation or overshoots.

The journal bearing clearance data shows that hydrodynamic bearing operation was reached by 300 rpm. The average clearance decreased for the first 2 seconds of operation (2000 rpm) then increased reaching 1.5 mils (38 μm) at 12 000 rpm.

There was negligible change in bearing operation passing through the critical speeds

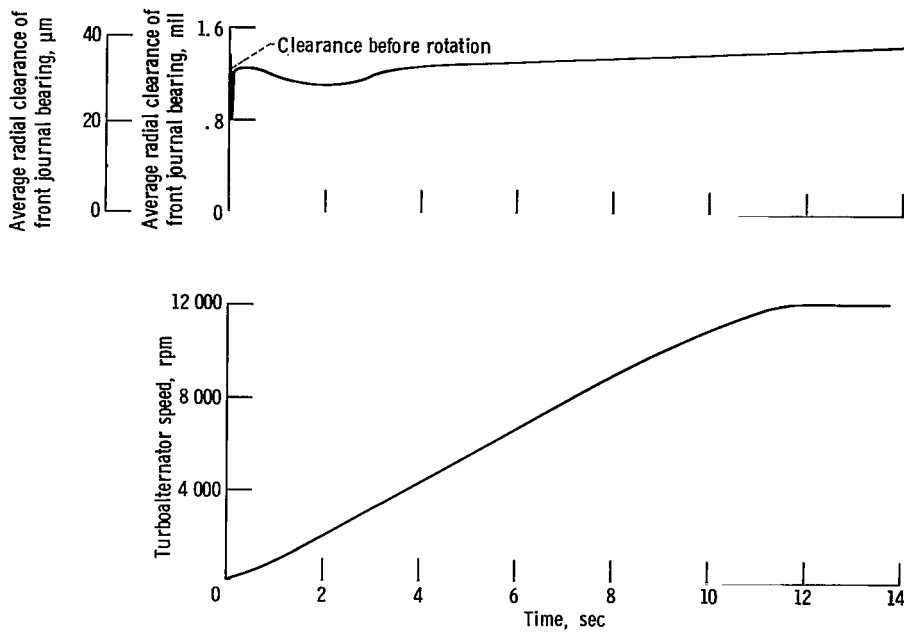


Figure 9. - Variation of front journal bearing average clearance and shaft speed with time during beginning of startup. Bearing support ring temperature, 125° F (324 K); bearing pad temperature, 105° F (313 K); assembled radial clearance, 0.8 mil (21 μ m).

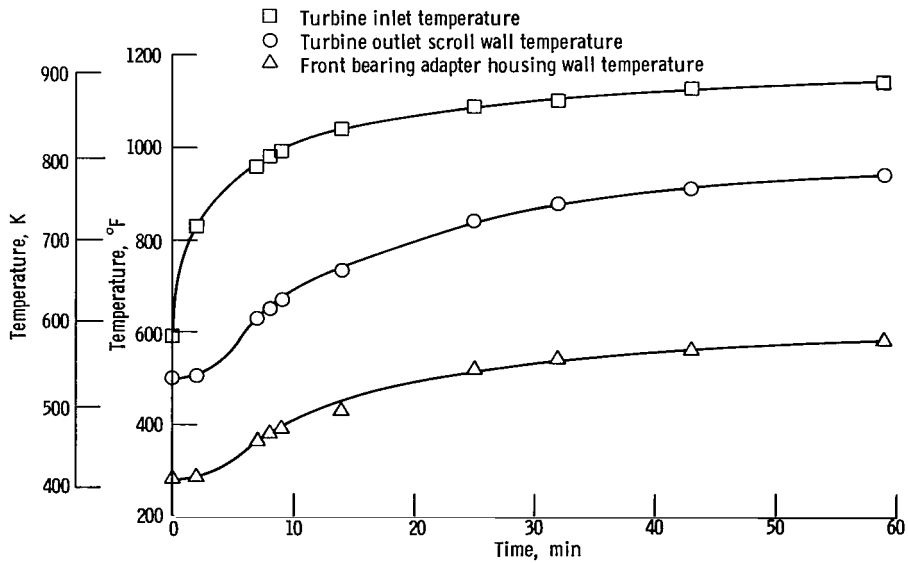


Figure 10. - Turbine temperature variation with time during fast startup.

(7200 to 9600 rpm); this was no doubt due to the speed of acceleration and the size of the criticals as reported in reference 20.

After reaching design speed, the thermal transient can be studied. Figure 10 shows how the turbine temperatures varied with time. Plotted along with gas temperature is the rear scroll wall temperature and the temperature of the adapter housing between the front journal bearing and the turbine housing. The profile of the wall and housing temperatures differ from the gas profile because of the thermal lag in heating the housings. The temperatures did not start at the same level because of conductive heating from the facility piping before the start of the test and after the insulation was replaced on the turbine. The long transient time can be attributed to the mass of the facility piping.

The effect of these thermal changes on temperature and clearances of the front bearing is shown in figure 11. Here the temperatures of the support ring for the bearing

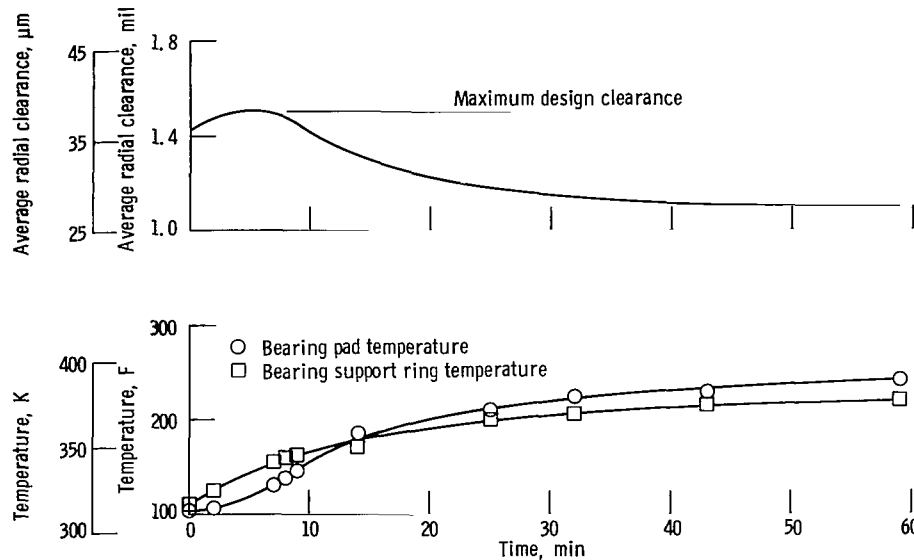


Figure 11. - Front bearing average clearance and temperatures experienced during startup transient.

pads and the pad temperatures are plotted along with radial bearing clearance. The pad temperature is indicative of the shaft temperature. The radial clearance is allowed by design to vary between 0.5 and 1.5 mils (13 and 38 μm). Figure 11 shows that the clearance started at the 1.43-mil (35-μm) value and got larger. The maximum clearance occurring 6 to 8 minutes into the startup. Even though the clearance slightly exceeded the design limit, the bearings continued to operate in a stable mode.

The clearance was large because of the thermal growth of the bearing support ring with respect to the shaft. The clearance continued to grow for a while because the ring

continued to heat up at a faster rate than the shaft. The profile of the pad temperature indicates a thermal lag while the support ring did not. The clearance began to decrease as the shaft began to heat up.

The support ring was heated conductively by the turbine and by oil in the heat exchanger passages. The shaft was heated by heat conducted from the turbine wheel and sheering of the gas film in the bearing. Figure 12 is a comparison of the temperature

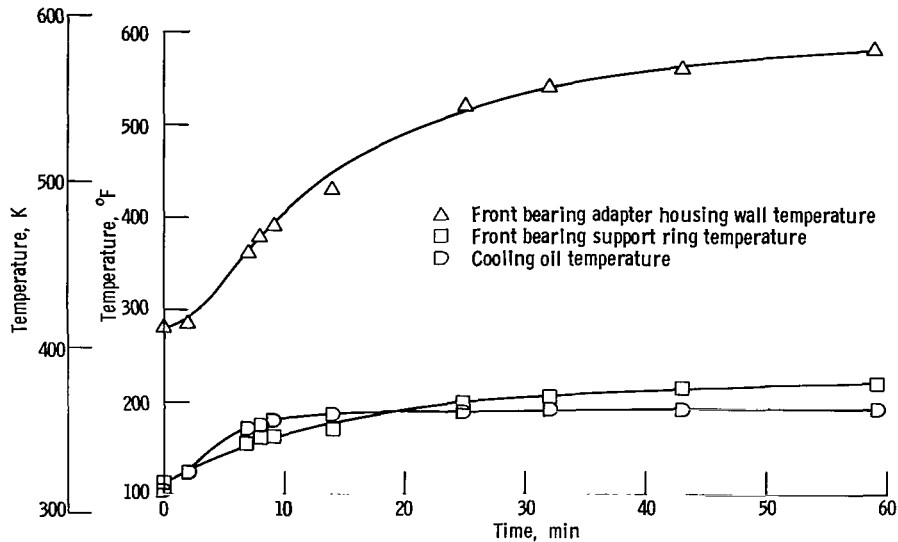


Figure 12. - Comparison of cooling oil temperature and adapter housing temperature to front bearing mount ring temperature during startup.

profiles of the adapter housing, the bearing support ring, and the cooling oil. The figure shows that the oil heated the bearing support ring rapidly, so it did not show the thermal lag that the adapter housing and the shaft temperature profiles showed.

Figure 13 shows the same parameters plotted for the rear bearing as was plotted for the front bearing in figure 11. As can be seen in the figure, the clearance values started at 1.5 mils ($38 \mu\text{m}$), then went downward. No oil was flowing through the support ring during this portion of the test. This indicates that the shaft temperature was raising faster than the support-ring temperature. After 4 minutes of operation, with clearance dropping at a fairly rapid rate and no signs of it leveling out, the operator started flowing oil through the support. As expected the clearance increased. But the increase was so rapid, that the operator shut off flow fearing that the clearance would get too high. When the clearance came back down it was allowed to continue, settling out at the 1-mil ($25\text{-}\mu\text{m}$) level without flowing any more oil through the support ring.

The temperature profile of the support ring is not plotted for the time interval between 2 and 7 minutes because exact data for the period were not available. Temper-

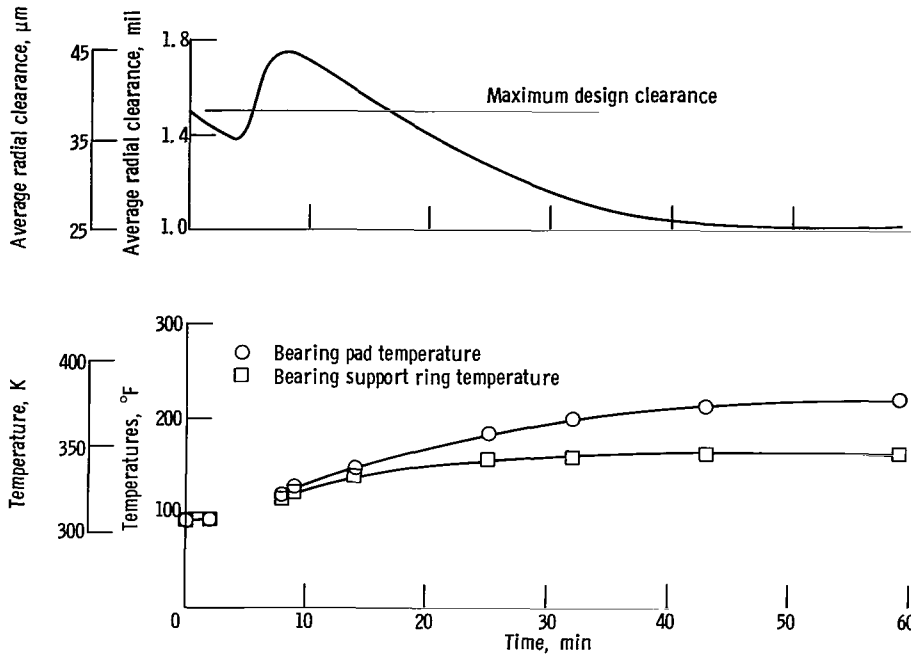


Figure 13. - Rear bearing average clearance and temperatures experienced during startup transient.

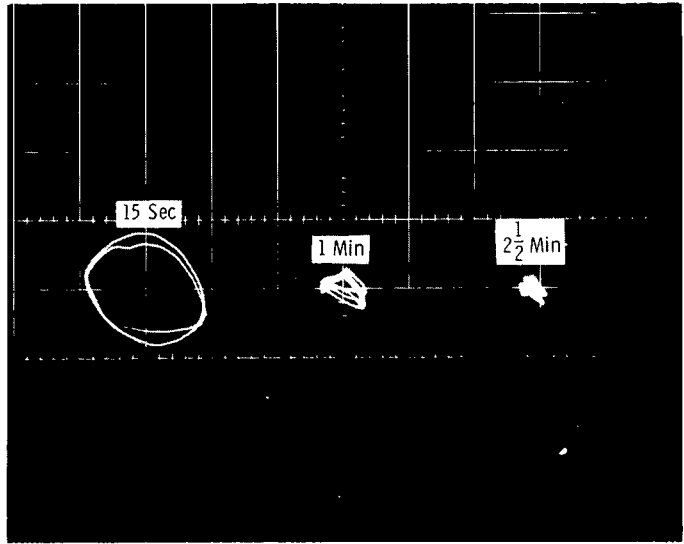
ature data were not recorded continuously as were bearing clearance data.

The most significant conclusion that can be drawn from this portion of the startup is that the journal clearance is very dependent on the support ring oil conditions.

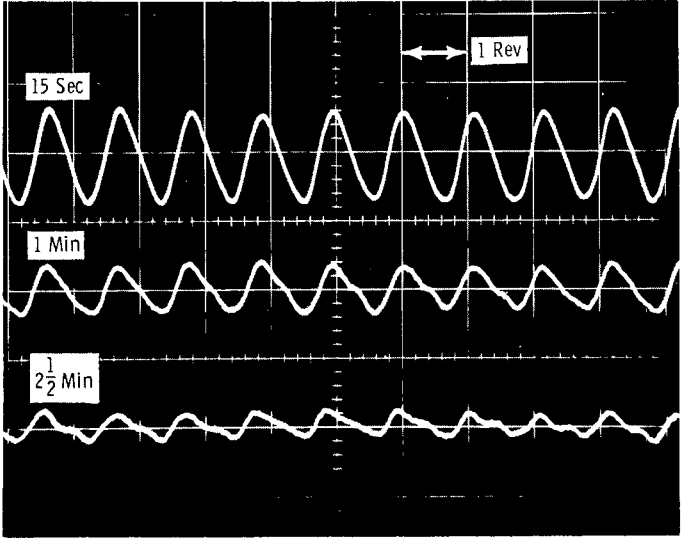
Reference 20 contains a figure showing journal clearance as a function of turbine inlet temperature. The curve shows the clearance of the front journal increasing with temperature but remaining within the $\frac{1}{2}$ - to $1\frac{1}{2}$ -mil (13 to 38 μm) operating envelope. At first glance, the data in this report appear to contradict this. But the data in reference 20 were taken at steady-state conditions where all thermal lags were allowed to settle out.

It was mentioned earlier that the bearing clearance was high at the beginning of the startup test but that the bearings operated stably. However, the motion of the shaft center (orbital motion) was higher than had been experienced in all other tests. The large orbit size was caused by the high starting clearance. As time passed the orbit got smaller reaching normal size after $2\frac{1}{2}$ minutes of operation. Photographs of the front bearing orbit are shown in figure 14. At the start the orbit size was 0.4 mil (1 μm) in diameter; the normal size was 0.1 mil (0.25 μm). The first trace in figure 14 (15-sec trace) was taken as soon as 12 000 rpm was reached.

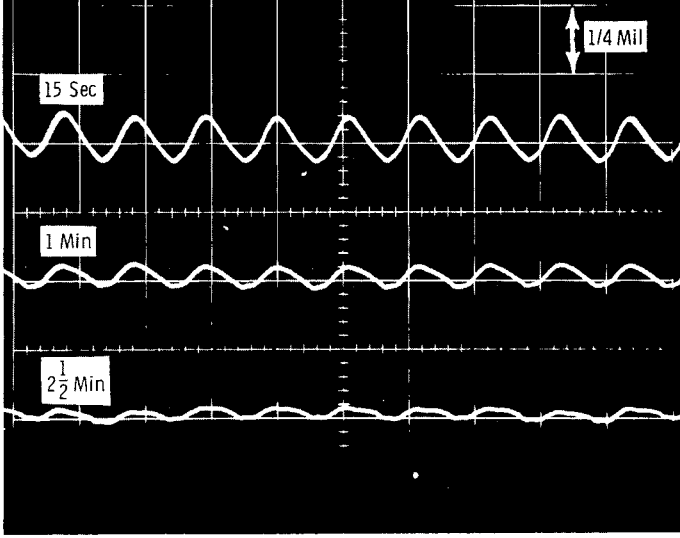
In addition to the orbits, figure 14 also shows photographs of the pitch and roll motion of the front journal bearing pads. The motions start out large, and their amplitude follows that of the orbit size. The largest motion shows no indication of any dis-



Orbital motion of front journal bearing.



Pad pitch motion.



Pad roll motion.

Figure 14. - Shaft and pad motions of front journal bearing during beginning of startup thermal transient.

turbance caused by physical contact with the shaft or by any sticking in the pivot ball and socket.

The thrust bearing was operated hydrostatically for the first 10 minutes of the transient, then operation was changed to the hydrodynamic mode. The changeover could have been made as soon as 12 000 rpm was reached, but it was delayed because of the unexpectedly large clearance experienced on the journal bearings. The thrust load remained constant during the thermal transient because the turbine inlet pressure and pressure ratio were constant. Thrust bearing operation was not affected by any thermal changes.

Change in Thrust Bearing Operational Mode

The turboalternator thrust bearing was designed with both hydrostatic and hydrodynamic capabilities. The hydrostatic capability was incorporated for startup to eliminate rubbing and to reduce starting torque. So the normal operating procedure was to start hydrostatically, then to switch to hydrodynamic operation when 12 000 rpm was reached. It should be noted here that this transient is part of the startup but is not thermal in nature.

A test was performed then to see how the bearings reacted to the change in operating mode. The test was made holding all conditions constant at design rating. The change in operating mode was made by either stepping on or off the external jacking gas supply used for hydrostatic operation. The gas pressures were 80 psi ($5.5 \times 10^5 \text{ N/m}^2$) on the main thrust and 100 psi ($6.9 \times 10^5 \text{ N/m}^2$) on the reverse thrust bearing.

Figure 15 shows how the main thrust bearing clearance is affected by the transients.

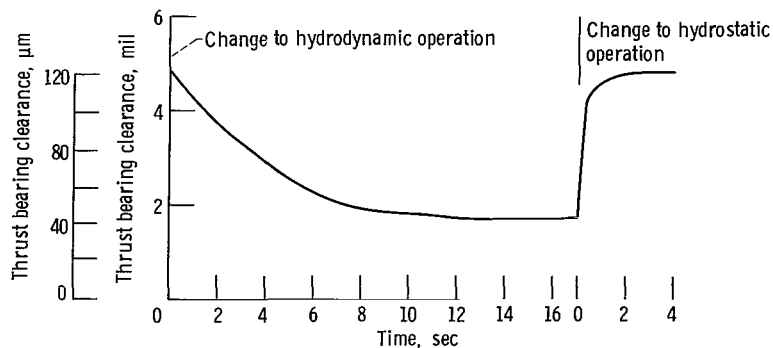


Figure 15. - Main thrust bearing clearance variation during transient from hydrostatic to hydrodynamic operation and back to hydrostatic.

The curve shows the change from hydrostatic to hydrodynamic operation then back to hydrostatic. The change to hydrodynamic operation is much slower because the jacking gas pressure is being bled down through small orifices in the thrust bearing stator faces (fig. 4). A secondary effect is the fact that the load capacity of the bearing is going from a pressure dependent state to a clearance dependent state. There were no other effects noticed on the turboalternator, including the journal bearings, while performing the thrust bearing mode transients. There was no instabilities, oscillation, or overshoots observed in the thrust bearings either.

Electrical Load Steps

The last tests to be discussed is the response of the gas bearing system (clearance changes) to electrical load transients. The load transients were applied by adding and removing load in steps. In all cases, the load was changed in step increments of approximately 3, 6, 9, and 12 kilowatts. The tests were conducted at the design shaft speed of 12 000 rpm at power factors of 0.8 lagging (design value) and approximately 1. The bearing cavity pressures were 6.3 psia (43 kN/m^2) for the front journal bearing, and 11.2 psi (77 kN/m^2) for the rear journal bearing and thrust bearing. The bearings were operated in the hydrodynamic mode throughout the tests.

Two types of load steps were studied: the stepping of the alternator load itself using the valve speed control and the stepping the useful load using the electric speed controller. Both types of speed controls represent methods considered for use in controlling turbine speed in an actual space power system. Even though the electrical system has been selected, the results of both methods are presented here.

The step changes using the valve speed control were of the load on-off-on type. They were made by first establishing the desired load level (or step size) on the alternator and the opening and closing contactor C1, leaving C3 open and C2 closed (see fig. 8). The resulting alternator power response is shown typically in figure 16. When contactor C1 is opened (on-off or load removal step), the alternator power drops off instantaneously as a pure step function. When contactor C1 is closed (off-on or load applied step), the alternator power increase is slower and is not a step function. Response curves of the gas bearing clearances will be presented for both steps.

Journal bearing clearance is the distance between the bearing pad and the journal (see fig. 3). The main thrust clearance is the distance between the thrust runner and the flexibly mounted main thrust stator (see fig. 4). The reverse thrust clearance is the distance between the thrust runner and the reverse thrust stator (fig. 4). The load step tests using valve speed control resulted in large clearance changes in both the main and reverse thrust bearings and negligible clearance changes in the journal bearings. The

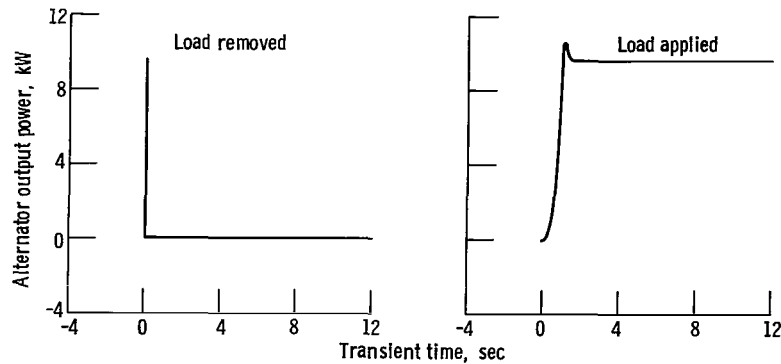


Figure 16. - Typical alternator output power response. Valve speed control: step load, 9.6 kilowatts; power factor, 0.8 lagging.

large clearance changes were a result of the change in turbine pressure ratio (aerodynamic thrust) caused by the turbine exhaust valve. The valve was controlling turbine power as a result of a sensed change in speed. So the thrust bearing reaction was an indirect result of the electrical load step and a direct result of the change in turbine pressure ratio.

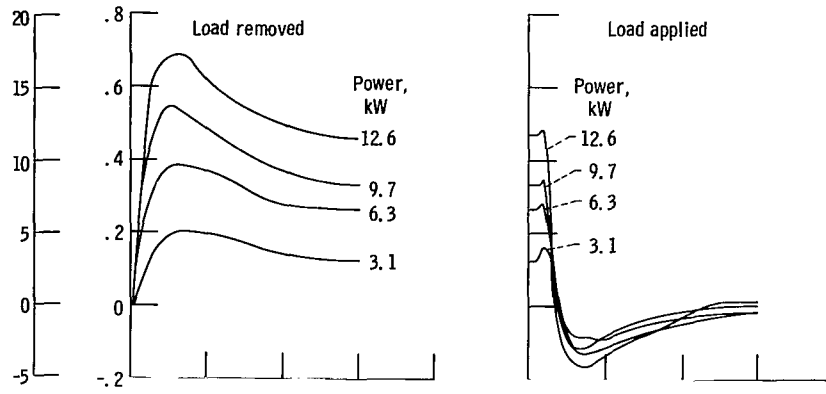
The response of the main and reverse thrust bearings to the steps is shown in figure 17. The data are presented in terms of change in clearance with respect to time for each transient. Zero change in clearance is the clearance the bearing was operating at before the transient was initiated. The largest changes that occurred were in the reverse thrust bearing, the maximum being 1.9 mils ($48 \mu\text{m}$) for the 12.6-kilowatt step.

The shape of the on-off (load removal) response curves for both the main and reverse thrust bearings approximate the response of a linear second-order system. For all step sizes the percent overshoot was constant at approximately 28 percent for the reverse thrust bearing and from 48 to 65 percent (within 20 percentage points of being constant) for the main thrust bearing. The difference in percent overshoot between the main and reverse thrust bearing shows that each is a separate system. This is expected because of the flexibly mounted main thrust stator. The relatively constant percent overshoot (independent of step size) of both thrust bearings indicate that each system is linear.

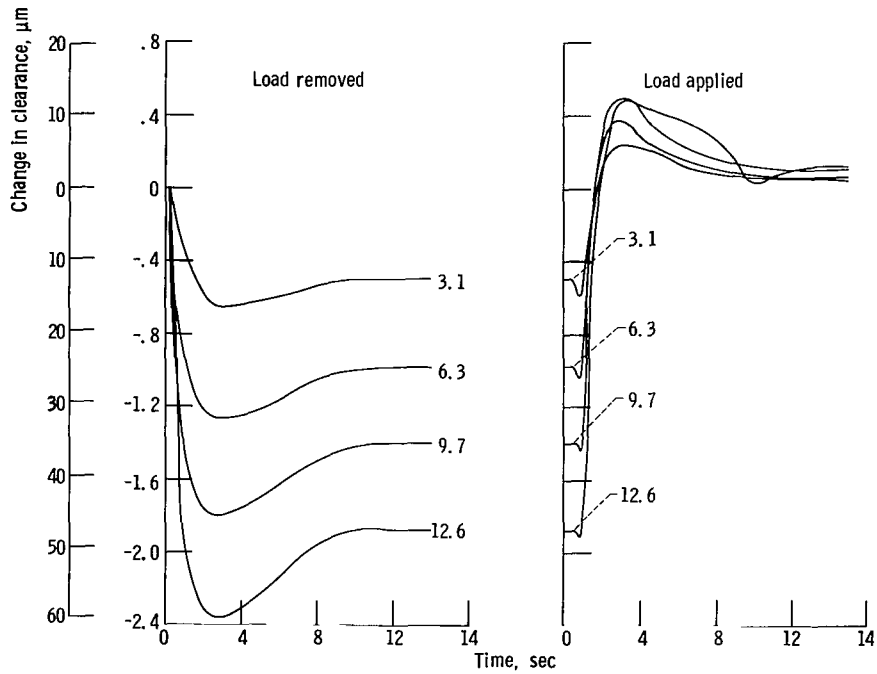
Another check for linearity of the thrust bearing responses is shown in figure 18 where maximum values of overshoot (clearance change) are plotted against step size. The resulting curve of each thrust bearing is a straight line. The maximum clearance change occurred for the 12.6-kilowatt step on the reverse thrust bearing. The clearance change is 2.4 mils ($60 \mu\text{m}$).

Based on these results, the reverse thrust bearing response approximates a linear second-order system with a damping ratio of 0.37 and a natural frequency of 0.25 hertz.

The load steps applied using the electric speed controller were done in a similar



(a) Main thrust bearing.



(b) Reverse thrust bearing.

Figure 17. - Transient response of thrust bearing system showing clearance change variation to on-off-on step changes in alternator power. Shaft speed, 12 000 rpm; power factor, 0.8 lagging; bearing cavity pressure, 11.2 psia ($7.7 \times 10^4 \text{ N/m}^2$); valve speed control.

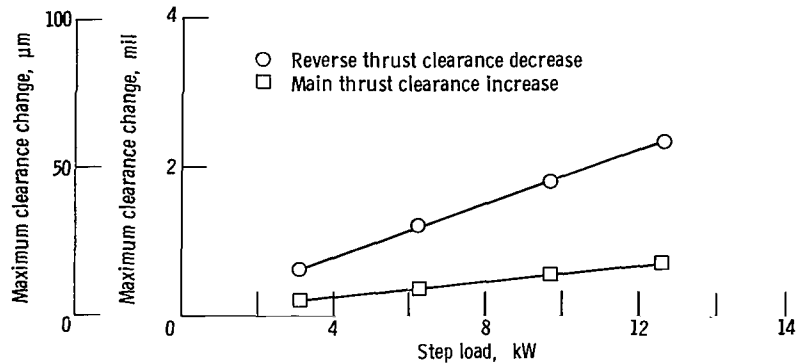


Figure 18. - Maximum overshoot in thrust clearance as function of step load change. Power factor 0.8 lagging; valve speed control.

manner. However, the transient was initiated using contactor C2; C1 and C3 were closed (fig. 8). These transients resulted in negligible clearance changes in both the thrust and journal bearings. Using this control system, the turbine ran at constant pressure ratio, thus power. Any changes in load were absorbed by the speed controller load bank. In other words, the speed controller added or removed load as necessary to maintain 12 000 rpm. As a result the thrust bearings did not see any load changes.

SUMMARY OF RESULTS

A gas bearing turboalternator built for a Brayton cycle power system underwent several different transient tests representative of the type expected in an actual system. The most significant results of the tests are as follows:

1. Journal bearing radial clearance increases over the design limit were experienced during an experimental startup. The large clearances were caused by insufficient control of the bearing mount ring coolant. The clearance is dependent on the mount ring coolant oil conditions. Although the clearances exceeded the design limit only slightly, they caused large bearing orbits. The bearings operated stably during the entire startup procedure.
2. The change from hydrostatic to hydrodynamic operation on the thrust bearing took place smoothly. The change back to hydrostatic operation was also smooth and took place in a shorter time when compared with the change to hydrodynamic operation.
3. Applying electrical step loads to the alternator using the turbine outlet pressure control valve to control the speed resulted in large but stable changes in thrust bearing

clearance and negligible changes in the journal bearings. Using the electrical speed control resulted in negligible changes to both the journal and thrust bearings.

Lewis Research Center,
National Aeronautics and Space Administration,
Cleveland, Ohio, August 21, 1970,
120-27.

REFERENCES

1. Bernatowicz, Daniel T.: NASA Solar Brayton Cycle Studies. Presented at the Symposium on Solar Dynamic Systems, Solar and Mechanical Working Groups of the Interagency Advanced Power Group, Washington, D. C. Sept. 24-25, 1963.
2. Kofskey, Milton G.; and Glassman, Arthur J.: Turbomachinery Characteristics of Brayton Cycle Space-Power-Generation Systems. Presented at the 9th Annual ASME Gas Turbine Conference and Products Show, Houston, Texas, Mar. 1-5, 1964.
3. Cohen, R.; Gilroy, W. K.; and Spencer, W. B.: High-Performance Turboalternator and Associated Hardware. I - Design of Turboalternator. NASA CR-1290, 1969.
4. Frost, A.; Lund, J. W.; and Curwen, P. W.: High-Performance Turboalternator and Associated Hardware. II - Design of Gas Bearings. NASA CR-1291, 1969.
5. Dryer, A. M.; Kirkpatrick, F. M.; Russell, E. F.; Wimsatt, J. M.; and Yeager, L. J.: Alternator and Voltage Regulator-Exciter for a Brayton Cycle Space Power System. Vol. I - Alternator and Voltage Regulator-Exciter Design and Development. Rep. GE-A69-003, General Electric Co., May 1969. (Work done under contract NAS3-6013).
6. Greenwell, J. E.; Russell, E. F.; and Yeager, L. J.: Alternator and Voltage Regulator-Exciter for a Brayton Cycle Space Power System. Vol. II - Unbalanced Electromagnetic Forces Investigation. Rep. GE-A69-003, General Electric Co., May 1969. (Work done under Contract NAS3-6013.)
7. Cohen R.; Gilroy, W. K.; and Havens, F. D.: Turbine Research Package for Research and Development of High Performance Turboalternator. Rep. PWA-2796, Pratt & Whitney Aircraft (NASA CR-54885), Jan. 1967.
8. Kofskey, Milton G.; and Nusbaum, William J.: Aerodynamic Evaluation of Two-Stage Axial-Flow Turbine Designed for Brayton-Cycle Space Power System. NASA TN D-4382, 1968.

9. Kofskey, Milton G.; and Nusbaum, William J.: Performance Evaluation of a Two-Stage Axial-Flow Turbine for Two Values of Tip Clearance. NASA TN D-4388, 1968.
10. Curreri, Joseph S.; Kruchowy, Roman; and Wood, James C.: Turbine Performance in a Gas-Bearing Brayton Cycle Turboalternator. NASA TN D-5604, 1969.
11. Edkin, Richard A.; Valgora, Martin E.; and Perz, Dennis A.: Performance Characteristics of a 15 kVa Homopolar Inductor Alternator for 400 Hertz Brayton Cycle Space-Power System. NASA TN D-4698, 1968.
12. Bollenbacher, Gary; Edkin, Richard A.; and Perz, Dennis A.: Experimental Evaluation of a Voltage Regulator-Exciter for a 15-Kilovolt-Ampere Brayton Cycle Alternator. NASA TN D-4697, 1968.
13. Word, John L.; Fischer, Raymond L. E.; and Ingle, Bill D.: Static Parasitic Speed Controller for Brayton-Cycle Turboalternator. NASA TN D-4176, 1967.
14. Fischer, Raymond L. E.; and Droba, Darryl J.: Dynamic Characteristics of Parasitic-Loading Speed Controller for 10-Kilowatt Brayton Cycle Turboalternator. NASA TM X-1456, 1968.
15. Corcoran, Charles S.; and Yeager, LeRoy J.: Summary of Electrical Component Development for a 400-Hertz Brayton Energy Conversion System. NASA TN D-4874, 1968.
16. Perz, Dennis A.; and Valgora, Martin E.: Experimental Evaluation of Volt-Ampere Loading and Output Distortion for a Turboalternator with Multiple Load Phase-Controlled Parasitic Speed Controller. NASA TN D-5603, 1969.
17. Valgora, Martin E.; and Perz, Dennis A.: Steady-State Electrical Performance of a 400-Hertz Brayton Cycle Turboalternator and Controls. NASA TN D-5658, 1970.
18. Wood, James C.; Valgora, Martin E.; Kruchowy, Roman; Curreri, Joseph S.; Preliminary Performance Characteristics of a Gas-Bearing Turboalternator. NASA TM X-1820, 1969.
19. Wood, James C.; Valgora, Martin E.; and Tryon, H. B.: Hot Performance Characteristics of a Gas Bearing Brayton Cycle Turboalternator. Proceedings of the Fourth Intersociety Energy Conversion Engineering Conference. AIChE, 1969, pp. 659-667.

20. Kruchowy, Roman; Wood, James C.; and Curreri, Joseph S.: Performance of a Turboalternator Gas-Bearing System at Steady-State Conditions. NASA TN D-5542, 1969.
21. Gilbert, Leonard J.: Reduction of Apparent-Power Requirement of Phase-Controlled Parasitically Loaded Turboalternator by Multiple Parasitic Loads. NASA TN D-4302, 1968.

FIRST CLASS MAIL



POSTAGE AND FEES PAID
NATIONAL AERONAUTICS AND
SPACE ADMINISTRATION

01U 001 28 51 3DS 70316 00903
AIR FORCE WEAPONS LABORATORY /WLOL/
KIRTLAND AFB, NEW MEXICO 87117

ATT E. LOU BOWMAN, CHIEF, TECH. LIBRARY

POSTMASTER: If Undeliverable (Section 158
Postal Manual) Do Not Return

"The aeronautical and space activities of the United States shall be conducted so as to contribute . . . to the expansion of human knowledge of phenomena in the atmosphere and space. The Administration shall provide for the widest practicable and appropriate dissemination of information concerning its activities and the results thereof."

— NATIONAL AERONAUTICS AND SPACE ACT OF 1958

NASA SCIENTIFIC AND TECHNICAL PUBLICATIONS

TECHNICAL REPORTS: Scientific and technical information considered important, complete, and a lasting contribution to existing knowledge.

TECHNICAL NOTES: Information less broad in scope but nevertheless of importance as a contribution to existing knowledge.

TECHNICAL MEMORANDUMS: Information receiving limited distribution because of preliminary data, security classification, or other reasons.

CONTRACTOR REPORTS: Scientific and technical information generated under a NASA contract or grant and considered an important contribution to existing knowledge.

TECHNICAL TRANSLATIONS: Information published in a foreign language considered to merit NASA distribution in English.

SPECIAL PUBLICATIONS: Information derived from or of value to NASA activities. Publications include conference proceedings, monographs, data compilations, handbooks, sourcebooks, and special bibliographies.

TECHNOLOGY UTILIZATION PUBLICATIONS: Information on technology used by NASA that may be of particular interest in commercial and other non-aerospace applications. Publications include Tech Briefs, Technology Utilization Reports and Notes, and Technology Surveys.

Details on the availability of these publications may be obtained from:

SCIENTIFIC AND TECHNICAL INFORMATION DIVISION
NATIONAL AERONAUTICS AND SPACE ADMINISTRATION
Washington, D.C. 20546